



Cite this: DOI: 10.1039/c9bm01932d

A sugar–lectin rich interface between soft tissue and the stiff byssus of *Atrina pectinata*†

Jimin Choi,  ‡^a Elise Hennebert,  ‡^b Patrick Flammang  *^c and Dong Soo Hwang  *^{a,d}

Maintaining durable adhesion between soft tissues and relatively hard implant materials is one of the most elusive technological difficulties in bionic devices due to contact damage between mechanically mismatched materials. Although there are many examples of coexistence of soft and hard tissues in living organisms, relatively little is known about the mechanisms used to overcome mechanical mismatches occurring at the interface between soft and hard tissues. Among the various creatures possessing mechanically mismatched biological tissues, *Atrina pectinata* is a good model system where the interface between stiff byssal threads and soft tissues is distributed all over an extended organ. In this study, we found a wide distribution of various types of carbohydrates and lectins at the mechanically mismatched interface of the byssus of *Atrina* using histological methods and proteomics. Reversible and robust interactions between the carbohydrate and lectins at the interface would play a major role in mitigating the contact damage at the *Atrina* interface. Based on these results, the adhesion between sugar and lectin would be useful to overcome a wide range of contact damage observed in research studies on bionic devices.

Received 30th November 2019,
Accepted 20th May 2020

DOI: 10.1039/c9bm01932d

rsc.li/biomaterials-science

Introduction

Increasing life expectancy and aging population are causing an increase in the demand for bionic devices and artificial organs to replace damaged body tissues.¹ Bionic devices and implantable materials such as prosthetic arms and legs² have dramatically improved the quality of life of differently abled persons. Significant progress in wearable electronics has allowed the fabrication of advanced bionic and artificial organs for the recovery of human sensory organs such as bionic ears or eyes to regaining movement of amputated limbs through neuroprosthetic devices.^{3,4}

However, for efficient use of bionic devices, it is necessary to overcome the problem of contact damage^{5,6} which may occur at the interface between relatively soft living tissues and stiff bionic devices⁷ due to mismatches in their mechanical properties such as hardness, stiffness, and Poisson's ratio. When an external mechanical stress is applied at the interface where soft human tissue meets a stiff bionic device, it is concentrated at the interface,⁸ causing cracks and eventually leading to adhesion failure between the surrounding tissue and the bionic device.⁹

The robust interconnection found in nature between living and non-living tissue components, usually involving different mechanical properties,⁸ is an attractive research area, especially for the development of bionic devices. Examples of such interconnection can be found between nails and fingers, shells and adductor muscles, bones and cartilage, and beaks and tendons. In nature, two strategies are used to mitigate contact damage that can occur at the stiff–soft interfacial junction: (A) strong interfacial adhesion,⁹ or (B) molecular gradient mechanical properties in the interfacial region.¹⁰ Examples of the former include tendon–muscle junctions,^{11,12} musculoskeletal systems,¹³ junctional collagen fibres and foam-like adhesive plaques in mussel byssus.¹³ The latter include dentin–enamel junctions¹⁴ and cementum–dentin junctions.¹⁵

In particular, the byssus, a fibrous holdfast produced by the fan shell, *Atrina pectinata*, can be used as a model system for

^aDivision of Integrative Biosciences and Biotechnology, Pohang University of Science and Technology (POSTECH), Pohang, 37673, Republic of Korea

^bCell Biology Unit, Research Institute for Biosciences, Université de Mons-UMONS, 7000 Mons, Belgium

^cBiology of Marine Organisms and Biomimetics Unit, Research Institute for Biosciences, Université de Mons-UMONS, 7000 Mons, Belgium.

E-mail: Patrick.Flammang@umons.ac.be

^dDivision of Environmental Science and Engineering, Pohang University of Science and Technology (POSTECH), Pohang, 37673, Republic of Korea.

E-mail: dshwang@postech.ac.kr

†Electronic supplementary information (ESI) available. See DOI: 10.1039/c9bm01932d

‡Both authors contributed equally to this work.

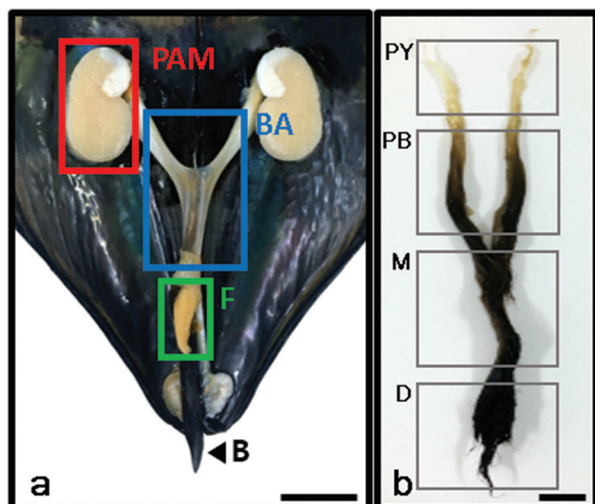


Fig. 1 Morphological features of the byssal system in *A. pectinata*. (a) Fan shell in which the adductor muscle has been cut in half to open the shell and the visceral mass has been removed to highlight the byssus and the byssal system. BA: byssal apparatus; B: byssus; F: foot, and PAM: posterior adductor muscle. (b) Byssus which has been removed from the byssal apparatus; PY: proximal yellow part; PB: proximal brown part; M: middle part; and D: distal part (scale bar = 2 cm).

studying loadbearing strategies where contact damage due to mechanical mismatch occurs. Similar to other well-known bivalve molluscs, fan shells firmly attach to the ocean bed by producing thread like structures collectively called byssus.^{16,17} In *Atrina*, the proximal part of the byssus penetrates deeply into soft body tissues so that it is securely anchored (Fig. 1a). Although this morphological arrangement may cause severe soft tissue damage due to the stiffness mismatch between the byssus and the soft tissue, the soft tissue damage does not occur in the affected area.^{9,17–19} Recently, *Atrina pectinata* foot protein 1 (apfp-1), a protein composed of two domains, a C-type lectin domain and a DOPA rich domain, has been identified to play a role in forming strong, reversible bonds in the interfacial region of *Atrina's* byssus.⁹ The uniqueness of the binding mechanism of apfp-1 is that the lectin–sugar binding provides a stronger binding force than the 3,4-dihydroxyphenylalanine (DOPA)–iron complex.^{9,20–22} Both sugar–lectin bonds and DOPA–iron complexes are well known to be widely used in underwater adhesion by marine organisms.^{23–25} Despite the high diversity of glycoconjugates and sugar-binding proteins, only one type of carbohydrate and lectin binding was investigated in our previous research.⁹ Therefore, in this study, the distribution of various sugars and lectins present at the interface between stiff byssus and soft surrounding tissues was examined. This required a prior description of the byssus-producing organs which had never been investigated in detail in this species. The knowledge of the interaction chemistry of different lectins and sugars could provide new relevant insights into ways to design a bionic interface for mitigating contact damage due to mechanical mismatch between soft surrounding tissues and bionic devices in tissue engineering and bionic applications.

Experimental

Sample collection and section preparation for histochemical analyses

Fan shell *Atrina pectinata* was obtained from Gangjin, South Korea. The byssus and the byssal system were carefully dissected and washed with fresh artificial seawater. They were fixed in 4% paraformaldehyde (PAF) in sodium phosphate buffer (PBS solution, pH 7.4), rinsed in PBS solution, dehydrated through an ethanol series, embedded in paraffin wax, and cut into 5 μm -thick sections with a microtome (Microm HM 340 E, ThermoFisher, Waltham, MA, USA).

Histological staining and histochemical tests

To describe the byssal system of *A. pectinata*, sections through different byssus-producing organs were stained with Heidenhain's Azan trichrome. The presence of glycoconjugates in the load-bearing system of *A. pectinata* was investigated by subjecting sections of different parts of the byssus and byssal system to periodic acid–Schiff (PAS) staining. Sections were also stained with 1% Alcian blue 8GX in 0.1N HCl (pH 1.0) or with 0.5% Alcian blue 8GX in 3% acetic acid (pH 2.5). Alcian blue is a cationic dye which shows a pH-dependent affinity for functional groups: at low pH (<1), it is specific for sulphated molecules, sulphates being the only ionized groups; while, at higher pH (>2.5), carboxylates are also ionized and both types of groups carry a negative charge.²⁶ All sections were observed using a Zeiss Axio Scope A1 microscope (Zeiss, Oberkochen, Germany) equipped with an Axiocam 305 digital camera.

Scanning electron microscopy (SEM)

PAF-fixed slices (0.5 mm in thickness) of the byssal system, comprising the byssus, were dehydrated in graded ethanol, then transferred to hexamethyldisilazane, and finally air dried. They were mounted on aluminium stubs, coated with gold–palladium in a sputter-coater and observed with a JEOL JSM-7200F field emission scanning electron microscope.

Lectin histochemistry

The presence of specific carbohydrate moieties in the load-bearing system of *A. pectinata* was tested using lectins, which are proteins or glycoproteins of nonimmune origin that can bind carbohydrates without chemical modification.²⁷ Six biotinylated lectins, purchased from Vector Laboratories (Burlingame, CA, USA), were used: Concanavalin A (Con A), *Dolichos biflorus* agglutinin (DBA), Soybean agglutinin (SBA), Wheat germ agglutinin (WGA), *Ulex europaeus* agglutinin I (UEA I), and *Ricinus communis* agglutinin I (RCA I).

Non-specific background staining was blocked by pre-incubation of sections in Tris-buffered saline, pH 8.0, containing 0.05% (v/v) Tween 20 and 3% (w/v) Bovine serum albumin (TBS-T-BSA). From this point on, all buffers were supplemented with 1 mM CaCl_2 and 1 mM MnCl_2 for Con A. Biotinylated lectins diluted at a concentration of 25 $\mu\text{g ml}^{-1}$ in TBS-T-BSA were applied on the sections for 2 h at room temperature. After 3 washes of 5 min in TBS-T, the sections

were incubated for 1 h in Texas-Red-conjugated streptavidin (Vector Laboratories) diluted 1 : 100 in TBS-T-BSA. Following 3 final washes of 10 min in TBS-T, they were mounted with Vectashield (Vector Laboratories). For lectins providing a positive labelling, control reactions were performed by substituting the lectins with TBS-T-BSA and by using lectins saturated with their inhibitory monosaccharides (0.4 M methyl α -D-mannopyranoside for Con A, 0.4 M *N*-acetyl-D-glucosamine or 0.2 M *N*-acetylneuraminic acid for WGA, and 0.4 M fucose for UEA I). Sections were observed using a Zeiss Axio Scope A1 microscope.

Protein identification

ESI-LC MS/MS was used for the profiling of proteins from the proximal and middle parts of the byssus (*i.e.* parts rooted in the mussel's tissues which comprise the byssus-tissue interfacial region). Carefully separated byssus-tissue interfacial region from the fan shell was briefly washed with deionized water. The proteins were extracted by sonication in 4 M urea, 5% acetic acid with 10 μ M leupeptin and pepstatin A (Sigma, St Louis, MO, USA) on ice.⁹ Thereafter, the proteins were concentrated and the solvent was changed to 50 mM Tris-Cl buffer (pH 7.4) using centrifugal filter units (Amicon ultra 3 K centrifugal filter unit, Millipore, USA). The proteins were slightly separated (over \sim 1 cm) on a 10% sodium dodecyl sulphate polyacrylamide gel electrophoresis (SDS-PAGE) gel and this portion of the gel lane was entirely cut into 6 successive sections.²⁸ In-gel trypsin digestion was performed on each gel piece. This approach was used to increase the chances of protein and PTM identification in ESI-LC MS/MS equipment by reducing the complexity of the protein sample as demonstrated in previous studies.^{28–30} Moreover, low molecular weight impurities detrimental to mass spectrometry experiments, including detergents and buffer components, can be removed during gel electrophoresis.²⁸

Reduction/alkylation of the samples was performed in 10 mM dithiothreitol (DTT, Sigma, St Louis, MO, USA) dissolved in 100 mM ammonium bicarbonate and incubated at 56 °C for 1 h. After cooling, the solutions were incubated at room temperature in 55 mM iodoacetamide (Sigma, St Louis, MO, USA) dissolved in 100 mM ammonium bicarbonate in the dark for 30 minutes. After this, the gel pieces were washed with 0.1 M ammonium bicarbonate, 50% v/v ammonium bicarbonate in acetonitrile, and acetonitrile for 5 minutes each. The proteins were digested with trypsin (MS grade, Pierce, ThermoFisher, Waltham, MA, USA) (enzyme to substrate ratio = 1 : 50) at 37 °C overnight. The resulting peptide samples were dried using Speed Vac and injected to ESI-MS/MS (Waltham, MA, USA).

All MS/MS spectra were analyzed using SEQUEST (ThermoFisher, Waltham, MA, USA; version 1.0). SEQUEST was set to search the transcriptome database of *A. pectinata* (unpublished, 20 025 entries) assuming that the peptides were generated with strict tryptic cleavage specificity. SEQUEST was searched with a fragment ion mass tolerance of 1.00 Da and a parent ion tolerance of 10.0 PPM. Carbamidomethylation of

cysteine was specified in SEQUEST as a fixed modification. Oxidation of methionine and acetylation of the N-terminus were specified as variable modifications. Scaffold (version Scaffold_4.10.0, Proteome Software Inc., Portland, OR) was used to validate MS/MS based peptide and protein identifications. Peptide identifications were accepted if they could be established at greater than 98.0% probability to achieve an FDR less than 0.1% by the Scaffold Local FDR algorithm. Protein identifications were accepted if they could be established at greater than 99.0% probability and contained at least 1 identified peptide. Protein probabilities were assigned by the Protein Prophet algorithm.³¹ Proteins that contained similar peptides and could not be differentiated based on MS/MS analysis alone were grouped to satisfy the principles of parsimony.

Results and discussion

Anatomy and morphology of the byssal system of *Atrina pectinata*

In terms of structure and synthesis of the byssus, the genus *Atrina* presents anatomical differences compared to genus *Mytilus* which has been frequently studied as a model for underwater adhesion. Whereas the byssal threads of *Mytilus* are short and connected to a stem rooted in the basal part of the foot,³² the byssal threads in *Atrina* are extremely long and pass through the entire body up to the posterior adductor muscles (Fig. 1a and 2a) The byssal system consists of two distinct parts: the foot, which can protrude through the shell aperture into the external environment, and an entirely internal, Y-shaped musculo-secretory organ, the byssal apparatus, which runs from the posterior end of the foot up to the posterior adductor muscles (Fig. 1a and 2a; see also (ref. 9)).

Atrina pectinata possesses the longest byssal threads among mussels,³³ measuring up to 20 cm in length. The distal part of the byssus is extruded outside the shell for external contact with the substratum. At this level, byssal threads are separate from each other. Conversely, in the middle and proximal parts of the byssus, threads are bound together by a matrix layer (Fig. 1b). Although the distal part of the byssus anchors the animal to the sediment,^{16,17} the middle and proximal parts are embedded in the byssal apparatus, leading to strong load bearing capacity in the harsh marine environment.

The foot has a conical shape and, when fully contracted, measures about 20 mm in length and ranges from 10 mm to 3 mm in diameter from its proximal part to its tip (Fig. 1a and 2a). A groove runs all along its ventral surface (Fig. 2a and b). Transverse sections show that most of the volume of the foot is occupied by muscle fibres (Fig. 2b). The Y-shaped byssal apparatus is hollow and contains a lumen which is an extension of the foot groove. Close to the foot, the lumen is roughly circular in shape (Fig. 2c) but becomes more star-shaped as one moves away from the foot (Fig. 2e and f). In the posterior paired branches of the byssal apparatus, the lumen becomes U-shaped (Fig. 2h). The byssal apparatus is highly muscularized, with many longitudinal muscle fibres running along its

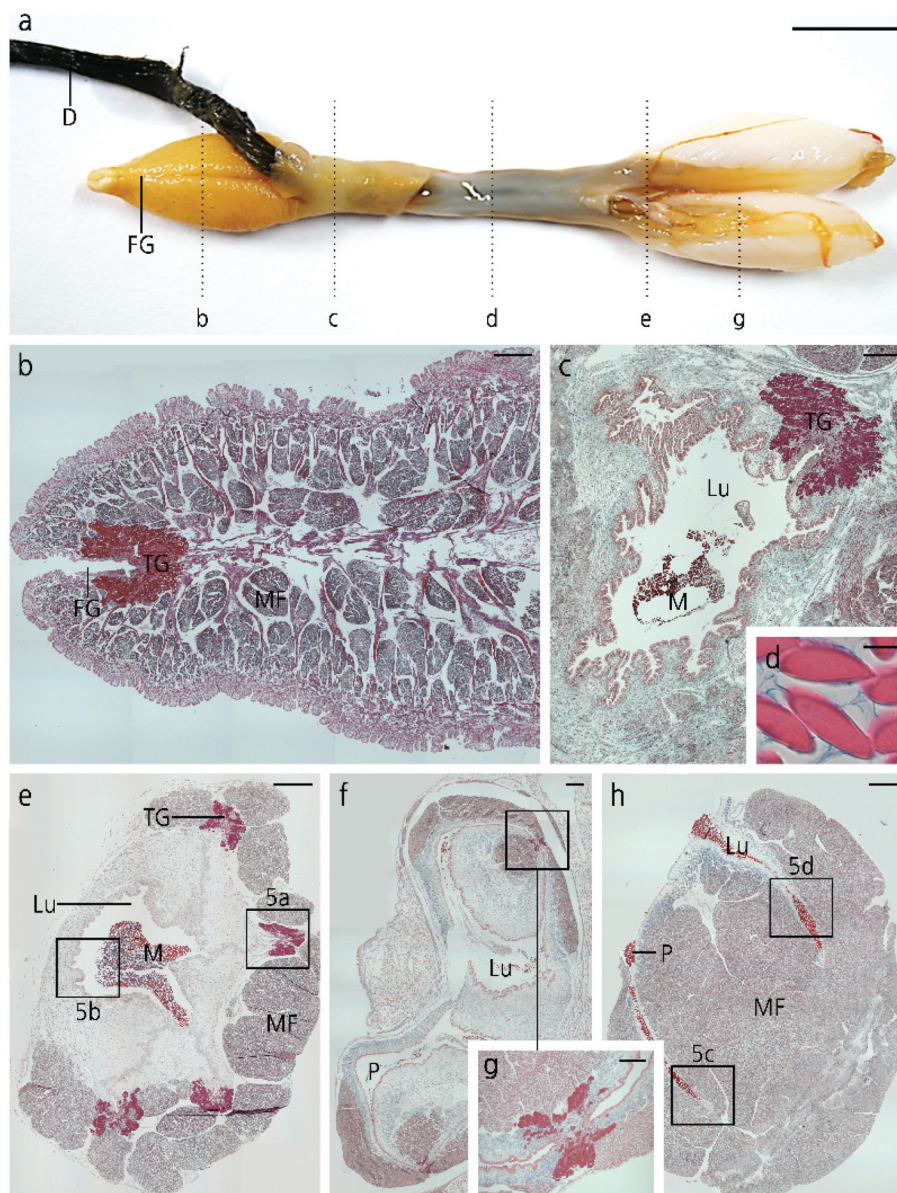


Fig. 2 The byssal system of *Atrina pectinata* (scale bars: 1 cm for a; 1 mm for b, c, e, f, and h; 20 μ m for d; and 250 μ m for g). (a) Whole byssal system, including byssal threads, dissected from a fan mussel. The dotted lines indicate transverse sections which were made in the foot (b), in the byssal apparatus just posterior to the foot (c), in the anterior branch of the byssal apparatus (e), at the Y junction (f), and in one of the paired posterior branches of the byssal apparatus (h). (d) Detail of the byssus showing the threads (in red) covered and interconnected by the matrix (in blue). (g) Detail of the thread gland as indicated in (e). D: distal part of the byssus, FG: foot groove, Lu: lumen, M: middle part of the byssus, MF: muscle fibres, P: proximal part of the byssus, and TG: thread gland.

lumen (Fig. 2). These muscles are particularly conspicuous in the posterior paired branches of the byssal apparatus (Fig. 2h).

Within the lumen, byssal fibres are embedded in a matrix which mediates cohesive interactions among them and with the surrounding tissues (Fig. 2d and h, Fig. 3 and 5). The matrix is intimately associated with the surface of the byssal threads as indicated by LM and SEM images (Fig. 2d and 3), suggesting strong interfacial interactions between the matrix phase and the thread material.

Different types of glands are involved in the synthesis of byssus: the thread gland and the matrix glands. The thread gland is a single, very long gland staining brightly red with tri-chrome stains (Fig. 2) and positively for catechol with Arnow staining, suggesting the presence of DOPA.³⁴ This gland lines the bottom of the foot groove (Fig. 2b) from the tip to the posterior part of the foot, then it extends into the byssal apparatus up to the anterior part of the paired branches (Fig. 2c–g). Within the byssal apparatus, the large gland first splits into four smaller glands, each located at the tip of the radial branches of the lumen (Fig. 2e). The two glands on each side

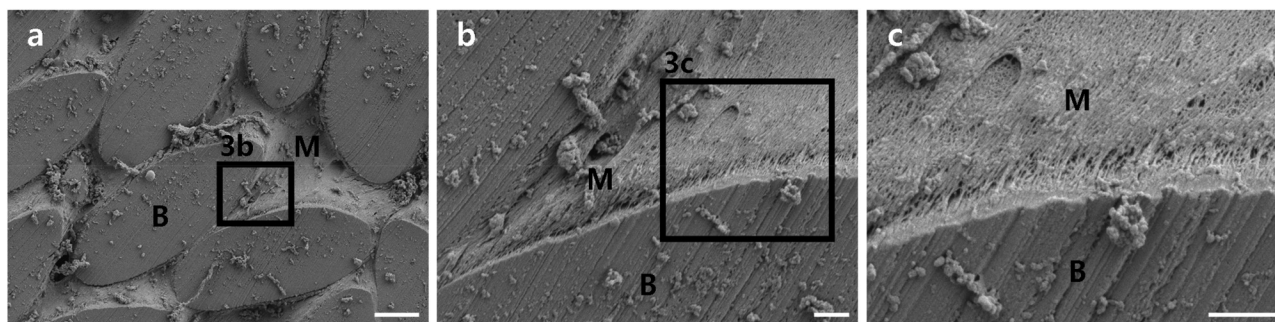


Fig. 3 Transverse section through the middle part of the byssus of *Atrina pectinata* observed by SEM (scale bars: 5 μm for a; and 1 μm for b and c). (a) A few threads embedded in a finely fibrillar matrix. (b and c) Details of the thread-matrix interface showing matrix nanofibrils intimately associated with the surface of the byssal threads. B: byssal thread and M: matrix.

of the byssal apparatus then come side by side at the Y junction (Fig. 2f and g). The thread glands finally end up in the anterior part of the paired branches. As indicated by its size, location and tinctorial affinity, the thread gland is responsible for the production of byssal fibres.

Matrix glands are not stained with trichrome stains but can be highlighted by histochemical stains such as periodic acid Schiff (PAS) and Alcian blue. At pH 2.5, Alcian blue stains carboxyl group-containing sugars (e.g. sialic acids, uronic acids, etc.), while at pH 1.0 it only stains sulphated glycosaminoglycans (GAGs) and glycoproteins.³⁵ PAS staining is primarily used for staining structures containing a high proportion of carbohydrates. Unlike Alcian blue staining, neutral carbohydrates are recognizable *via* PAS staining because this method recognizes the structure of monosaccharide units (vicinal diols) instead of detecting acidic groups of glycoconjugates. All these methods stain the matrix surrounding the byssal threads in the middle and proximal parts of the byssus, suggesting that it contains neutral sugars as well as sulphated and carboxylated sugars. Based on histochemical staining, two types of matrix glands can be recognized in the byssal apparatus (Fig. 5): the large matrix gland, an Alcian blue positive gland made up of large subepithelial cells surrounding the main lumen of the anterior branch (Fig. 5b) or clustered at the base of the thread gland (Fig. 5a); and the small matrix gland, a PAS positive gland consisting of smaller subepithelial cells lining the narrow lumen processes all along the byssal apparatus (Fig. 5a and d). Both glands extend over the entire length of the byssal apparatus, even in the most posterior part where the thread gland is no longer present (Fig. 2h and 5c, d).

Identification of carbohydrates within the byssus and byssal apparatus of *A. pectinata*

The carbohydrate fraction of the byssus was investigated using 6 biotinylated lectins (SBA, WGA, Con A, UEA I, RCA I, and DBA). Two of them, WGA and Con A, were strongly reactive to the proximal yellow and brown parts of the byssus while a weaker labelling was obtained with UEA I (Table 1, Fig. 4). In all three cases, the carbohydrate fraction was located in the matrix surrounding the byssal threads. The labelling of the middle part of the byssus with Con A and WGA was restricted

Table 1 Summary of the reactivity of the byssus and byssal apparatus of *Atrina pectinata* to ConA, WGA and UEA I. + and – indicate the presence or absence of labelling, respectively. LMG: large matrix gland, M: middle part, PY: proximal yellow part; PB: proximal brown part, SMG: small matrix gland, and TG: thread gland

	Byssus			Byssal apparatus			
	PY	PB	M	SMG ant.	SMG post.	LMG	TG
Con A	+	+	+ ^a	+	+	+	+
WGA	+	+	+ ^a	+	+	+	+
UEA I	+	+	–	–	+	–	–

^a Labelling of matrix fragments attached to the byssal threads.

to small areas around the fibers. No labelling was obtained with UEA I for this part of the byssus. The labelling obtained with Con A and UEA I completely disappeared when they were pre-incubated with their hapten monosaccharides (methyl α -D-mannopyranoside and fucose, respectively). The inhibition of WGA labelling was only partial when this lectin was pre-incubated with either *N*-acetyl-D-glucosamine or *N*-acetylneuraminic acid (sialic acid).

The three lectins that labelled the byssus (ConA, WGA and UEA I) were then used to stain the carbohydrates in the byssal apparatus (Table 1, Fig. 5). The labelling of the matrix within the tissue corresponds to that of the byssus after dissection (Fig. 4). However, the quasi absence of the matrix surrounding the threads in the middle part of the byssus suggests that the area illustrated in Fig. 5a and b is more posterior compared to that shown in Fig. 4 (middle). Similarly, the strong staining with UEA I indicates that the area shown in Fig. 5c and d corresponds to the proximal brown part of the byssus. The thread gland was labelled with Con A and WGA, but not with UEA I. The labelling obtained with Con A was completely inhibited by pre-incubation of the lectin with methyl α -D-mannopyranoside. Sialic acid completely inhibited the labelling with WGA while partial labeling was observed after pre-incubation with *N*-acetyl-D-glucosamine. A similar reactivity to the three lectins was observed for the large matrix glands, although in that case *N*-acetyl-D-glucosamine completely inhibited WGA labelling while sialic acid did not. Regarding small

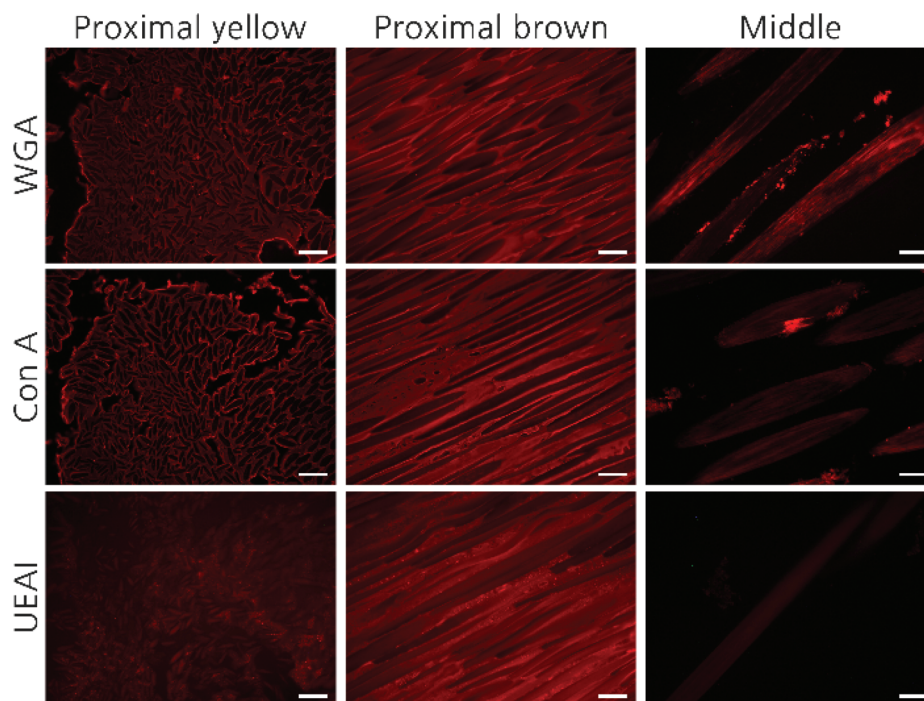


Fig. 4 Lectin labelling in different parts of the byssus of *Atrina pectinata*. Reactive structures are labelled with red (scale bar = 50 μm).

matrix glands, their reactivity to the lectins varied along the byssal apparatus. In the posterior branches, they were labeled with the three lectins, while in the anterior branches the reactivity to UEA I was absent. A complete inhibition of labelling was observed when the lectins were incubated with their hapten monosaccharide and, in this case, both *N*-acetyl-D-glucosamine and sialic acid inhibited WGA.

The lectin staining confirmed that both types of matrix glands are involved in the synthesis of the matrix of the byssus as identical sugar residues were detected in the glands and in the matrix of the byssus. Among the three lectins strongly labelling the matrix of the byssus, Con A recognizes mannose residues present as part of a “core oligosaccharide” in many glycoproteins, UEA I binds to glycoproteins containing terminal fucose residues, and WGA targets oligosaccharides containing terminal *N*-acetylglucosamine structures or sialic acid residues.²⁴ WGA can also bind some polysaccharides and proteoglycans. Together with the results from histochemistry, lectin staining therefore demonstrates that the matrix of the byssus contains both glycoproteins and sulphated proteoglycans, some of these glycoconjugates are sialylated. Considering that both proximal (yellow and brown) and middle parts of the byssus, because they are embedded in the byssal apparatus, must face tissue damage by mechanical mismatch, the glycoconjugate-rich matrix surrounding the byssal fibres and connecting them to the tissue is likely involved in energy dissipation to mitigate such contact damage. The presence of carbohydrate-binding protein partners such as apfp-1 would therefore allow the strong anchorage of the byssal threads in the matrix.

Identification of carbohydrate-binding proteins in the byssus–tissue interfacial region

To identify the proteins with a sugar binding domain at the byssus–tissue interface, the proteins on the surface of the proximal part of the byssus were carefully harvested, slightly separated by SDS-PAGE and subjected to tryptic digestion, and the resulting peptides were analysed by electrospray ionization–liquid chromatography–tandem mass spectrometry (ESI-LC-MS/MS). All MS/MS samples were analysed using SEQUEST (Thermo Fisher Scientific, San Jose, CA, USA; version 1.0) and the program was set to search the transcriptome database of *A. pectinata* (20 025 entries). The search results of MS/MS spectra were filtered with a significance threshold of $P < 0.05$ and the annotated MS/MS spectra were manually inspected to remove false positive. The complete results of the proteomic analysis are presented in the ESI Table S1.†

The NCBI's Conserved Domain Search Service (CD-search) was used to determine the proteins with carbohydrate-binding domains.³⁷ The amino acid sequences of carbohydrate-binding proteins and the location of the carbohydrate-binding domain are presented in the ESI.† The functional domain annotation and its accession number are presented in Table 2 for each sugar-binding protein. Besides, the number of unique peptides which corresponds to peptides that exist only in one protein of a proteome of interest,³⁶ and the coverage indicating the percentage of amino acids identified in MS/MS result are shown in Table 2. Since the coverage can be high in a low molecular weight protein even though the number of identi-

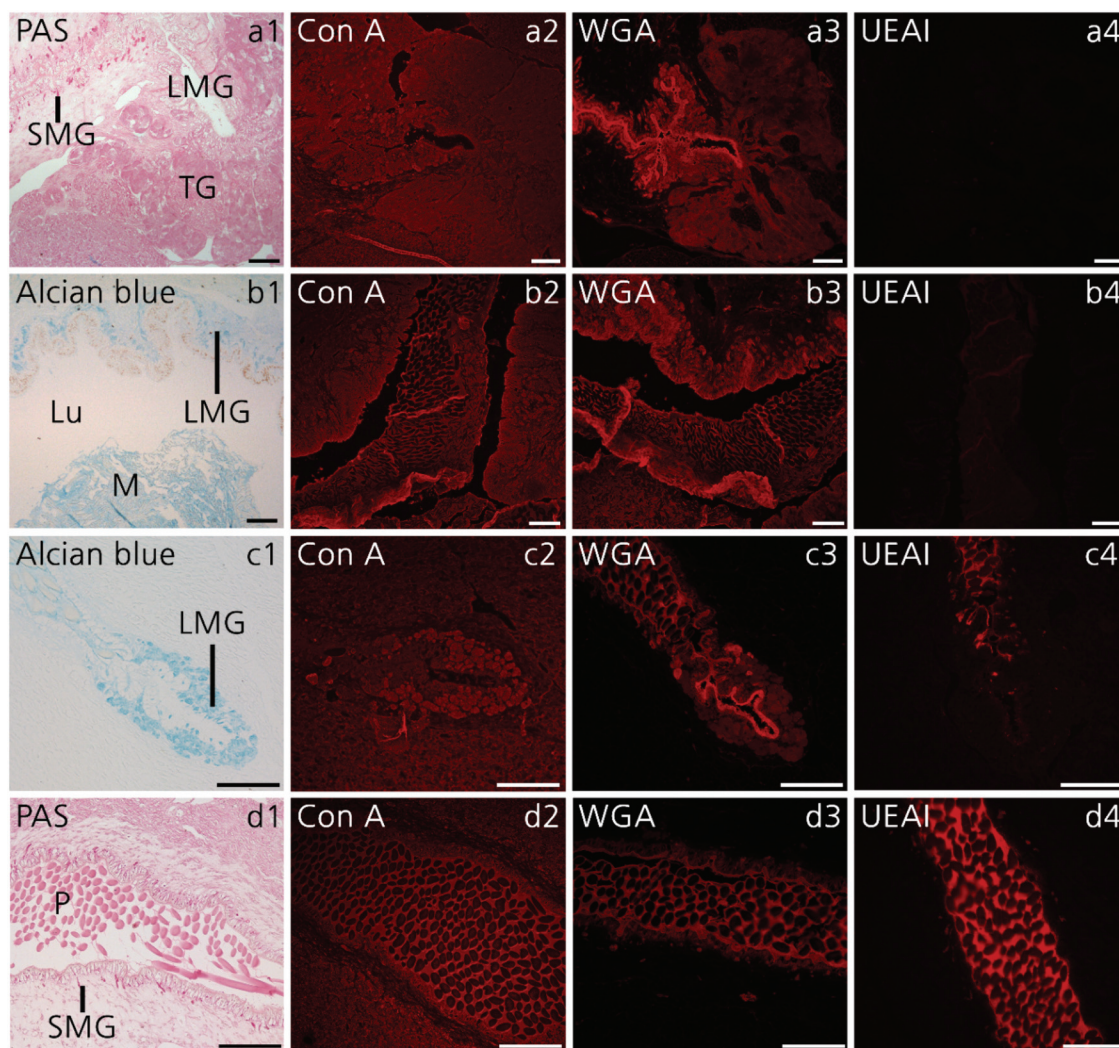


Fig. 5 Distribution of carbohydrate-containing molecules in the anterior (a and b) and posterior (c and d) branches (as indicated in Fig. 2) of the byssal apparatus of *Atrina pectinata*. Histochemical staining (1) and lectin staining using Con A (2), WGA (3) and UEA I (4). LMG: large matrix gland, Lu: lumen, M: middle part of the byssus, P: proximal part of the byssus, SMG: small matrix gland, and TG: thread gland.

Table 2 The list of proteins identified with ESI-LC-MS/MS in the byssus-tissue interfacial region and the carbohydrate-binding domain

Accession number of transcriptome	No. of unique peptide	Protein sequence coverage (%)	Molecular weight [kDa]	Functional annotation	Accession of functional annotation	e-Value of CD-search
m.14349 * foot protein 1 [<i>Atrina pectinata</i>]	6	16	36	C-type lectin(CTL) or carbohydrate-recognition domain(CRD)	smart00034	1.72×10^{-25}
m.8455	6	18	63	Galactoside binding lectin	smart00908	7.31×10^{-37}
m.9790	5	22	32	C-type lectin (CTL)/C-type lectin-like (CTL) domain	cl02432	7.07×10^{-4}
m.14568	3	13	28	Galactoside-binding lectin	smart00908	1.87×10^{-35}
m.15895	3	17	35	C-type lectin (CTL)/C-type lectin-like (CTL) domain	cd00037	3.85×10^{-7}
m.8438	4	7	95	C-type lectin (CTL)/C-type lectin-like (CTL) domain	cl28897	2.31×10^{-89}
m.8549	2	8	28	C-type lectin (CTL)/C-type lectin-like (CTL) domain	cd00037	3.65×10^{-29}
m.218	3	16	26	C-type lectin (CTL)/C-type lectin-like (CTL) domain	cd00037	2.75×10^{-29}
m.14097	2	10	29	C-type lectin (CTL)/C-type lectin-like (CTL) domain	cd00037	2.33×10^{-8}
m.12209	6	38	25	NTR_like domain ^a	cl02512	1.43×10^{-37}
m.2564	3	37	16	DOMON_like superfamily ^b	cl14783	3.37×10^{-17}
m.1338	3	49	14	WSC domain ^c	pfam01822	1.25×10^{-17}

^a NTR_like domain; a beta barrel with an oligosaccharide/oligonucleotide-binding fold. ^b DOMON_like superfamily; a diverse group of ligand binding domain which have been shown to interact with sugar and hemes. ^c WSC domain; domain expected to be involved in carbohydrate binding.

fied amino acids is low, the molecular weight of each protein is additionally listed.

The result presented in Table 2 shows that many carbohydrate-binding proteins in the interfacial region have a C-type lectin domain (CTLN). It is noteworthy that not only *A. pectinata* foot protein-1 (apfp-1, m.14 349), the interfacial region protein with a CTLNs reported in the previous report,⁹ but also many other proteins (m.9790, m.15 895, m.8438, m.8549, m.218, and m.14 097) with CTLNs were found. In addition, proteins with the galactose binding lectin domain (m.8455 and m.14 568), NTR like domain (m.12 209), DOMON like superfamily (m.2564), and WSC domain (m.1338) were also detected (Table 2). These results suggest that many proteins with lectin domains are localized on the surface of the byssus of *Atrina*, and that their lectin domains are likely to interact with the carbohydrate-rich matrix.

Conclusions

In this study, we performed biochemical analyses of *Atrina pectinata*'s loadbearing system to understand how to overcome mechanical mismatches at the interface where soft tissues meet relatively hard byssus. Histological analysis, including carbohydrate detection using conventional staining and lectin binding assay, confirmed that the carbohydrate-rich matrix was generally present at the interface surrounding the stiff byssus of *Atrina*. Remarkably, these surface sugars do not exist in the distal part of the byssus where energy dissipation is unnecessary as a result of it not being in contact with the tissue and exiting to the outside. In addition, the absence of carbohydrate-rich matrix in the distal part of the byssus may also be related to minimizing unnecessary biofouling on the distal part of the byssus. Previous studies on the formation of biofilms by bacteria have revealed that there are proteins that act as lectins on the surface of bacteria and that the biofouling mechanism proceeds by lectin recognition of the sugar on the substrate.^{38,39} Therefore, *Atrina* seems to prevent the degradation of biomaterial caused by bacterial biofilm formation by not exposing carbohydrates on parts of the byssus where they are not necessary.

Furthermore, proteome analysis showed that proteins that show homology with proteins functioning as lectin, which binds specifically to sugars, are abundantly distributed throughout the interface where the mechanical mismatch occurs. Considering the strong and reversible interactions between lectin and sugar found at the site of stiff-soft interface shown in the previous study,⁹ it is expected that several types of sugars and lectins form complex strong and reversible bonds at the interface between the stiff byssus and the soft surrounding tissue, thereby dissipating contact damage occurring at the interface. Besides, if the lectin and carbohydrate-rich interface can be artificially designed, it is expected to effectively mitigate the contact damage occurring in the tissue engineering field using the bionic-body devices.

Conflicts of interest

There are no conflicts to declare.

Acknowledgements

This work was supported by the National Research Foundation of Korea (NRF) funded by the Ministry of Science and ICT (NRF-2016M1A5A1027594 and NRF-2019M3C1B7025093), and by a KONNECT Bilateral European-Korean Seed Grant (NRF-2015K1A3A1A59074243 (KR); FNRS ERA-NET no. R.50.16.16.F (BE)). P. F. is the Research Director of the FRS-FNRS, Belgium.

Notes and references

- 1 R. Hinchet and S.-W. Kim, *ACS Nano*, 2015, **9**, 7742–7745.
- 2 J. Jagur-Grodzinski, *Polym. Adv. Technol.*, 2006, **17**, 395–418.
- 3 S. S. Srinivasan, M. Diaz, M. Carty and H. M. Herr, *Sci. Rep.*, 2019, **9**, 1981.
- 4 Y. Zou, P. Tan, B. Shi, H. Ouyang, D. Jiang, Z. Liu, H. Li, M. Yu, C. Wang and X. Qu, *Nat. Commun.*, 2019, **10**, 1–10.
- 5 D.-H. Kim and D. C. Kim, *Nat. Electron.*, 2018, **1**, 440–441.
- 6 C. Dagdeviren, *Science*, 2016, **354**, 1109–1109.
- 7 J. H. Zettl, E. M. Burgess and R. Romano, *Contract*, 1970, **5261**, 1–6.
- 8 B. Bar-On, F. G. Barth, P. Fratzl and Y. Politi, *Nat. Commun.*, 2014, **5**, 3894.
- 9 H. Y. Yoo, M. Iordachescu, J. Huang, E. Hennebert, S. Kim, S. Rho, M. Foo, P. Flammang, H. Zeng and D. Hwang, *Nat. Commun.*, 2016, **7**, 1–8.
- 10 J. D. Fox, J. R. Capadona, P. D. Marasco and S. J. Rowan, *J. Am. Chem. Soc.*, 2013, **135**, 5167–5174.
- 11 E. Evans, M. Benjamin and D. Pemberton, *J. Anat.*, 1990, **171**, 155.
- 12 M. Benjamin, E. J. Evans and L. Copp, *J. Anat.*, 1986, **149**, 89–100.
- 13 H. Zhao and J. H. Waite, *Biochemistry*, 2006, **45**, 14223–14231.
- 14 V. Imbeni, J. Kruzic, G. Marshall, S. Marshall and R. Ritchie, *Nat. Mater.*, 2005, **4**, 229–232.
- 15 S. P. Ho, S. J. Marshall, M. I. Ryder and G. W. Marshall, *Biomaterials*, 2007, **28**, 5238–5245.
- 16 T. Pearce and M. LaBarbera, *J. Exp. Biol.*, 2009, **212**, 1449–1454.
- 17 J. Mascolo and J. Waite, *J. Exp. Zool.*, 1986, **240**, 1–7.
- 18 M. J. Harrington and J. H. Waite, *J. Exp. Biol.*, 2007, **210**, 4307–4318.
- 19 K. J. Coyne, X.-X. Qin and J. H. Waite, *Science*, 1997, **277**, 1830–1832.
- 20 M. J. Harrington, A. Masic, N. Holten-Andersen, J. H. Waite and P. Fratzl, *Science*, 2010, **328**, 216–220.
- 21 N. Holten-Andersen, M. J. Harrington, H. Birkedal, B. P. Lee, P. B. Messersmith, K. Y. C. Lee and J. H. Waite, *Proc. Natl. Acad. Sci. U. S. A.*, 2011, **108**, 2651–2655.

- 22 H. Zeng, D. S. Hwang, J. N. Israelachvili and J. H. Waite, *Proc. Natl. Acad. Sci. U. S. A.*, 2010, **107**, 12850–12853.
- 23 F. Zeng, J. Wunderer, W. Salvenmoser, T. Ederth and U. Rothbächer, *Philosophical Transactions of the Royal Society B*, 2019, **374**, 20190197.
- 24 E. Hennebert, R. Wattiez and P. Flammang, *Mar. Biotechnol.*, 2011, **13**, 484–495.
- 25 P. Flammang, A. Michel, A. Cauwenberge, H. Alexandre and M. Jangoux, *J. Exp. Biol.*, 1998, **201**, 2383–2395.
- 26 M. Gamble and J. Bancroft, *Luna LG Manual of histologic staining methods of the Armed Force Institute of pathology*, MC Grow Hill Book company, Newyork, 3rd edn, 2001.
- 27 A. Leatham and N. Atkins, *J. Clin. Pathol.*, 1983, **36**, 747–750.
- 28 A. Shevchenko, H. Tomas, J. Havli, J. V. Olsen and M. Mann, *Nat. Protoc.*, 2006, **1**, 2856.
- 29 J. Shin, M. Kim, H.-J. Jung, H. L. Cha, H. Suh-Kim, S. Ahn, J. Jung, Y. Kim, Y. Jun and S. Lee, *Sci. Rep.*, 2017, **7**, 1–11.
- 30 H. Wang, T. Chang-Wong, H.-Y. Tang and D. W. Speicher, *J. Proteome Res.*, 2010, **9**, 1032–1040.
- 31 A. I. Nesvizhskii, A. Keller, E. Kolker and R. Aebersold, *Anal. Chem.*, 2003, **75**, 4646–4658.
- 32 C. Brown, *J. Cell Sci.*, 1952, **3**, 487–502.
- 33 D. Pasche, N. Horbelt, F. Marin, S. Motreuil, E. Macias-Sanchez, G. Falini, D. S. Hwang, P. Fratzl and M. J. Harrington, *Soft Matter*, 2018, **14**, 5654–5664.
- 34 L. E. Arnow, *J. Biol. Chem.*, 1937, **118**, 531–537.
- 35 M. R. Green and J. V. Pastewka, *J. Histochem. Cytochem.*, 1974, **22**, 774–781.
- 36 Y. Zhao and Y.-H. Lin, *Genomics, Proteomics Bioinf.*, 2010, **8**, 33–41.
- 37 A. Marchler-Bauer, Y. Bo, L. Han, J. He, C. J. Lanczycki, S. Lu, F. Chitsaz, M. K. Derbyshire, R. C. Geer and N. R. Gonzales, *Nucleic Acids Res.*, 2017, **45**, D200–D203.
- 38 M. A. Schembri and P. Klemm, *Infect. Immun.*, 2001, **69**, 1322–1328.
- 39 S. M. Abdel-Aziz and A. Aeron, *SAJ Biotechnol.*, 2014, **1**, 1–10.